



## Original Research Article

## The applicability of empirical vegetation indices for determining leaf chlorophyll content over different leaf and canopy structures

H. Croft<sup>a,\*</sup>, J.M. Chen<sup>a</sup>, Y. Zhang<sup>b</sup><sup>a</sup> University of Toronto, Department of Geography, Toronto M5S 3G3, Canada<sup>b</sup> Division of Biological and Physical Sciences, Delta State University, Cleveland, MS 38733, USA

## ARTICLE INFO

## Article history:

Received 24 June 2013

Received in revised form 25 October 2013

Accepted 12 November 2013

Available online 12 December 2013

## Keywords:

Remote sensing

Reflectance

Leaf area index

Modelling

Needleleaf

Broadleaf

Leaf biochemistry

## ABSTRACT

Retrieving leaf chlorophyll content at a range of spatio-temporal scales is central to monitoring vegetation productivity, identifying physiological stress and managing biological resources. However, estimating leaf chlorophyll over broad spatial extents using ground-based traditional methods is time and resource heavy. Satellite-derived spectral vegetation indices (VIs) are commonly used to estimate leaf chlorophyll content, however they are often developed and tested on broadleaf species. Relatively little research has assessed VIs for different leaf structures, particularly needle leaves which represent a large component of boreal forest and significant global ecosystems. This study tested the performance of 47 published VIs for estimating foliar chlorophyll content from different leaf and canopy structures (broadleaf and needle). Coniferous and deciduous sites were selected in Ontario, Canada, representing different dominant vegetation species (*Picea mariana* and *Acer saccharum*) and a variety of canopy structures. Leaf reflectance data was collected using an ASD Fieldspec Pro spectroradiometer (400–2500 nm) for over 300 leaf samples. Canopy reflectance data was acquired from the medium resolution imaging spectrometer (MERIS). At the canopy level, with both leaf types combined, the DD-index showed the strongest relationship with leaf chlorophyll ( $R^2 = 0.78$ ; RMSE =  $3.56 \mu\text{g}/\text{cm}^2$ ), despite differences in leaf structure. For needleleaf trees alone the relationship with the top VI was weaker ( $D_{\text{red}}$ ,  $R^2 = 0.71$ ; RMSE =  $2.32 \mu\text{g}/\text{cm}^2$ ). A sensitivity study using simulated VIs from physically-modelled leaf (PROSPECT) and canopy (4-Scale) reflectance was performed in order to further investigate these results and assess the impacts of different background types and leaf area index on the VIs' performance. At the leaf level, the MNDVI8 index showed a strong linearity to changing chlorophyll and negligible difference to leaf structure/type. At canopy level, the best performing VIs were relatively consistent where LAI  $\geq 4$ , but responded strongly to differences in background at low canopy coverage (LAI = 2). This research provides comprehensive assessments for the use of spectral indices in retrieval of spatially-continuous leaf chlorophyll content at the leaf (MTCI:  $R^2 = 0.72$ ;  $p < 0.001$ ) and canopy (DD:  $R^2 = 0.78$ ;  $p < 0.001$ ) level for resource management over different spatial and temporal scales.

© 2013 Elsevier B.V. All rights reserved.

## 1. Introduction

The amount of solar radiation absorbed by a leaf is largely a function of the foliar concentrations of photosynthetic pigments, with Chlorophyll *a* and *b* playing a crucial role in the conversion of solar radiation into stored chemical energy through photosynthesis. Consequently, low chlorophyll concentrations can directly limit photosynthetic potential and hence primary production (Richardson et al., 2002). This pivotal role of chlorophyll in photosynthesis and net primary productivity is therefore a driving force for obtaining spatially-continuous chlorophyll content inputs at a variety of spatial and temporal scales to regional and global

carbon models (Inoue, 2003). Foliar chlorophyll is strongly related to leaf nitrogen content (Daughtry et al., 2000) and acts as a bio-indicator of plant physiological condition; highlighting regions of plant disturbance and stress (Gitelson et al., 2003; Sampson et al., 2003). Understanding differences in the physiological response of leaf chlorophyll to changing biotic and abiotic factors between and within species is also important to resource management (Richardson et al., 2002). The accurate retrieval chlorophyll content at different spatiotemporal scales is crucial for the effective monitoring and understanding a number of ecosystem responses. Remote sensing plays a unique role in the ability to provide spatially-continuous data at fine temporal intervals and across broad spatial extents.

Leaf reflectance is controlled by the presence of foliar constituents such as chlorophyll, nitrogen, carotenoids, and water (Ustin et al., 2004). In visible wavelengths, chlorophyll absorbs

\* Corresponding author. Tel.: +1 4169783375.

E-mail address: [holly.croft@utoronto.ca](mailto:holly.croft@utoronto.ca) (H. Croft).

strongly in red and blue spectral regions, with maximum absorbance between 660 and 680 nm and maximum reflectance in green wavelengths (560 nm). Internal leaf structure also affects the amount of incident radiation absorbed, scattered and reflected through the upper epidermis, due to refractive discontinuities between intercellular air spaces and cell walls (Blackburn, 2006). Broadleaves have a thin epidermal layer, long palisade cells and more air spaces surrounding spongy mesophyll cells, whereas cylindrical needle leaves have an undifferentiated, densely packed mesophyll and thick cell walls (Ollinger, 2011). Research has suggested that NIR reflectance is controlled by the ratio of mesophyll cell surface to intercellular air spaces (Serrano, 2008). As such, differences in needleleaf and broadleaf reflectance spectra could exist even with the same chlorophyll content; making chlorophyll content estimation across plant functional types complex. At the canopy level, reflectance is also governed by leaf architecture, leaf area index (LAI), clumping, leaf angle distribution, tree density, non-photosynthetic canopy elements (Croft et al., 2013; Demarez and Gastellu-Etchegorry, 2000; Simic et al., 2011), along with solar/viewing geometry, ground cover and understory vegetation (Broge and Leblanc, 2001). Conifer canopies reflect less NIR radiation than broadleaf canopies, which is a function of the optical properties of the leaves, non-photosynthetic elements and leaf angle distribution. Vertical leaves promote a deeper penetration of incident radiation within the canopy, where multiple scattering within the crown allows for a higher probability of photon absorption (Ollinger, 2011). It is also therefore possible that reflectance factors from two forest canopies are different even if the spectral reflectance of the constituent leaves is the same (Blackburn, 1998).

Empirical spectral vegetation indices (VIs) are perhaps the most popular and straightforward means of retrieving chlorophyll content from reflectance factors. Spectral indices are formulated using ratios of wavelengths that are sensitive to a particular leaf pigment or to spectral regions where scattering is mainly driven by leaf internal structure or canopy structure (Blackburn, 2006). Recent research has focussed on improving the generality and applicability of spectral indices, through testing and modification over a range of species and physiological conditions, using empirical and simulated data (Blackburn, 2006). Most VIs are based on reflectance from wavelengths in the visible, NIR and around the red-edge, although some also contain exclusively visible wavelengths (Filella et al., 1995; Gitelson et al., 2002). Sims and Gamon (2002) analyzed nearly 400 leaf samples from 53 species, finding that leaf surface reflectance was an important factor in weak relationships between VIs and chlorophyll content. Le Maire et al. (2004) found that a modified simple ratio (mSR705) accounted for surface scattering on an experimental database (53 leaves) and a simulated database (>11,000 spectra), although the VI showed a dependence on leaf water content (Serrano, 2008). Whilst there has been considerable research devoted to deriving statistical relationships between leaf optical properties and chlorophyll content, they have often been developed and tested using a few closely related species, at the leaf scale and under controlled laboratory conditions (Blackburn, 1998; Gamon and Surfus, 1999; Gitelson et al., 2003; Le Maire et al., 2004). Fewer studies still have addressed the effect of leaf anatomical characteristics on leaf and canopy reflectance and chlorophyll content estimation (Serrano, 2008). It is important to assess the accuracy of VIs across different functional scales, leaf structures, and with additional canopy variables for their implementation within a reliable forest management programme. This is particularly relevant for trees with needle leaves, which have seen little focus or investigation in terms of using VIs to derive leaf chlorophyll content. Most studies relating empirical vegetation indices to chlorophyll content have focussed on broadleaves, at

either the leaf or canopy scale, limiting their application and validation to specific plant functional types and observational scales.

This paper will assess the performance of VIs within and across leaf types and at different spatial sampling units (leaf and canopy), using empirical data and simulated data from radiative transfer models. The simulation of leaf and canopy data through physical models (PROSPECT; Jacquemoud and Baret, 1990 and 4-SCALE; Chen and Leblanc, 1997) allows the testing of a greater range of chlorophyll values and canopy conditions, including the important influence of background composition and leaf area index. It also helps to validate and better understand the performance of VIs for the empirical dataset. A fundamental notion is to investigate how well these current techniques can be applied across species and leaf structures, in order to assess the contribution of other variables at leaf and canopy levels.

The specific aims of this research are to:

- i. evaluate the accuracy of a comprehensive set of empirical indices for retrieving chlorophyll content from different leaf structures (broadleaf and needleleaf);
- ii. assess the ability of empirical indices to predict leaf chlorophyll content at leaf-level from ground based measurements and canopy-level from remotely sensed data;
- iii. determine the sensitivity of VIs to chlorophyll content across different LAI values and background contributions.

## 2. Methods

### 2.1. Field locations and data collection

Two field locations were selected representing broadleaf deciduous and needleleaf coniferous vegetation sites. Field sampling was conducted in 2004 in a mature broadleaf sugar maple (*Acer saccharum* M.) stand located in Haliburton Forest, Ontario Canada (45°14'16" N, 78°32'18" W). Haliburton forest falls within the Great-Lakes – St.-Lawrence region (Rowe, 1972), with an average annual precipitation of approximately 1050 mm and mean annual temperature of 5 °C (Gradowski and Thomas, 2006). The upland hardwood forests of Haliburton Forest are dominated by sugar maple but also contain beech (*Fagus grandifolia* Ehrh.), eastern hemlock (*Tsuga canadensis* (L.) Carr.), and yellow birch (*Betula alleghaniensis* Britt.) (Caspersen and Sapruff, 2005). The site is underlain by shallow brunisols or juvenile podzols, (pH 4.2–5.1); mainly silty sands from Precambrian Shield granite or granite-gneiss deposits (Gradowski and Thomas, 2006). Ground-based measurements were carried out 8 times throughout the growing season from 27th May to 30th September, which are indicated in Table 1 by the day of year (DOY) within the site ID (see Zhang et al., 2007 for a more detailed description). Leaf samples were collected from the top of tree crowns within a 50 m × 20 m area, considered to be representative of the stand.

Eight sites in a coniferous forest located northwest of Sudbury, Ontario (46°49'13" N to 47°12'9" N and 81°22'2" W to 81°54'30" W) were sampled in the summer of 2003 and 2004 (Zhang et al., 2008a,b). The sites contain mature black spruce (*Picea mariana*) stands of different ages, crown closures and health condition, underlain by shallow soils on Canadian Shield bedrock. Leaf samples were taken from the top of tree canopies within a 20 m × 20 m area considered representative of the selected stands. Temperatures range from –40 °C to 30 °C and average summer rainfall is 71.3 mm, with snow-covered ground from December to March (Rayfield et al., 2005). Other local tree species include jack pine (*Pinus banksiana*) and Aspen (*Populus tremuloides* Michx.). Table 1 details the study sites used in this research, including their

**Table 1**

Site locations, structural parameters and vegetation type and condition. Haliburton site IDs refer to the day of year that ground sampling was conducted.

Location	Site ID	Location	Vegetation	LAI	$\Omega$	Condition
Haliburton	Ha157	45°14'16" N, 78°32'18" W	Broadleaf	–	–	Healthy
	Ha164	45°14'16" N, 78°32'18" W	Broadleaf	4.12	0.86	Healthy
	Ha193	45°14'16" N, 78°32'18" W	Broadleaf	7.15	0.90	Healthy
	Ha199	45°14'16" N, 78°32'18" W	Broadleaf	–	–	Healthy
	Ha214	45°14'16" N, 78°32'18" W	Broadleaf	5.45	0.98	Healthy
	Ha246	45°14'16" N, 78°32'18" W	Broadleaf	–	–	Healthy
	Ha263	45°14'16" N, 78°32'18" W	Broadleaf	5.34	0.94	Healthy
	Ha275	45°14'16" N, 78°32'18" W	Broadleaf	4.86	0.93	Healthy
	Sudbury 2003 and 2004	Sb2	47°12'08" N, 81°54'29" W	Needle	3.97	0.81
Sb3		46°49'17" N, 81°22'06" W	Needle	2.36	0.88	Stressed
Sb4		46°49'13" N, 81°22'30" W	Needle	3.21	0.84	Stressed
Sb5		46°54'27" N, 81°25'11" W	Needle	3.09	0.80	Healthy
Sb6		47°09'52" N, 81°44'32" W	Needle	3.78	0.77	Healthy
Sb7		47°09'45" N, 81°44'32" W	Needle	1.14	0.85	Stressed
Sb8		47°09'45" N, 81°43'37" W	Needle	2.88	0.84	Stressed
Sb9		47°11'58" N, 81°52'01" W	Needle	3.83	0.84	Healthy

locations. The selected sites represent a range of canopy structural conditions (LAI and foliage clumping index ( $\Omega$ )), leaf types and vegetation health.

### 2.1.1. Leaf reflectance and biochemistry

Leaf reflectance factors and leaf chlorophyll content ( $\mu\text{g}/\text{cm}^2$ ) were measured from a total of 247 broadleaf samples and 86 needleleaf samples, collected from the sites and dates listed in Table 1. Leaves and shoots were sampled from the upper canopy using a shotgun and leaf reflectance and transmittance measured using an ASD spectroradiometer Fieldspec Pro FR (Analytical Spectral Devices, Inc. Boulder, USA) attached via a fibre optic cable to a Li-Cor 1800 integrating sphere (Li-Cor 1800-12S, Li-COR, Inc., Lincoln, Nebraska, USA). Reflectance and transmittance spectra were measured using methods described by Harron (2000) and Zhang et al. (2007). Needle leaves were placed in specially designed black anodized carriers to take spectral measurements (Harron, 2000; Zhang et al., 2008b). Broadleaf leaves were clamped to the sample port on the sphere wall. Leaf samples were sealed in plastic bags and kept at a temperature of 0 °C for subsequent chlorophyll (Chl  $a + b$ ) analysis, using the method reported by Moorthy et al. (2008). For comparison with the canopy level study, ground leaf chlorophyll values were calculated for each site as average values from the within-site samples collected.

### 2.1.2. Structural parameters

Canopy architecture can play a perturbing role in modelling leaf chlorophyll content from reflectance factors (Blackburn, 1998). Leaf area index and canopy structural parameters are important parameters needed in the inversion of canopy radiative transfer models. Effective LAI ( $L_e$ ) was measured using the LAI-2000 plant canopy analyser (Li-Cor, Lincoln, NE, USA) (see Chen et al., 1997, for more details). The clumping index was measured using TRAC (Tracing Radiation and Architecture of Canopies) (Chen and Cihlar, 1995). Clumping index values quantify the non-random spatial distribution of foliage, with a lower value indicating increased foliage clumping. Based on ground measurements, Chen et al. (1997) found that Black Spruce stands have an average clumping index of 0.84, in comparison to Jack Pine of 0.68. Broadleaf forests have less clumping and values approach unity.

## 2.2. Satellite data acquisition and processing

### 2.2.1. MERIS data

MERIS is a medium-spectral resolution imaging spectrometer, sampling surface reflectance in fifteen spectral bands from 415–885 nm, with a temporal revisit time of 2–3 days. Ten MERIS Full

Resolution Level 2 (300 m) images were used in this study, covering all dates and study sites in Table 2. The L2 products also contain geolocated geophysical parameters, including geometric information, solar and viewing geometry, terrain height, some meteorological data and image quality flags (Canisius et al., 2010). MERIS Level 2 (L2) products were radiometrically and atmospherically corrected for Rayleigh scattering, ozone, water vapor absorption and aerosol content. The MERIS images were reprojected to WGS 84 and coordinate system (UTM 18) and resampled using nearest neighbour interpolation using the BEAM VISAT software application (European Space Agency). The images were also co-registered and geometrically corrected using a grid of tie points, which were distributed evenly throughout the image and contained geo-location coordinates.

### 2.2.2. Wavelength interpolation

As MERIS has a limited number of narrow wavebands, cubic-spline spectral interpolation was performed at 1 nm wavelength intervals in order to calculate VIs at the correct wavelengths, following the procedure of Canisius and Fernandes (2012). All MERIS bands apart from the oxygen (760.625 nm) and water absorption (900 nm) bands were used in the spectral interpolation. Canisius and Fernandes (2012) investigated the accuracy of MERIS spectral interpolation using VIs calculated from Hyperion data against VIs calculated from cubic spline interpolation of MERIS equivalent Hyperion reflectance. The interpolation of MERIS equivalent Hyperion reflectance agreed with Hyperion reflectance within 5%, with the exceptions of wavelengths between 580 nm to 590 nm and 690 nm to 700 nm (Canisius and Fernandes, 2012). VIs calculated using these wavelengths were still included in this research, however, results from this limited number of VIs may be affected by interpolation and contain a higher degree of uncertainty.

## 2.3. Spectral vegetation indices

The main types of indices are derived from three forms; simple ratio (SR), normalized difference (ND), and red edge, with modified versions of SR and ND having developed to correct for leaf surface reflectance. SR and ND indices usually contain a reference wavelength between 750–900 nm to account for vegetation structure and an index wavelength (often between 660–720 nm) that is sensitive to the pigment of interest (Sims and Gamon, 2002). Vegetation indices can also be comprised of derivative spectra; calculated as the slope of reflectance spectra, and have been suggested to correct for variation in leaf surface scattering and BRDF effects and background reflectance (Vogelmann et al., 1993).

**Table 2**

Details of all published spectral indices tested in this study. RI = reflectance index.

Index	Name	Equation	Reference
BGI	Blue green pigment index	$(R450/R550)$	Zarco-Tejada et al. (2005)
BI	Brightness index	$(R800 + R670 + R550)/\text{SQRT}(3)$	Liu and Moore (1990)
CI	Colouration index	$(R800-R550)/R800$	Liu and Moore (1990)
CTR	Carter index	$R695/R760$	Carter (1994)
CUR	Curvature index	$(R675 \times R690)/R683^2$	Zarco-Tejada et al. (2001)
DD	Datt derivative	$D(754)/D(704)$	Datt (1999)
Datt99	Datt 99	$(R850-R710)/(R850-R680)$	Datt (1999)
DVI	Difference VI	$R800-R670$	Jordan (1969)
$D_{[\text{red}]}$	Derivative reflectance at D690	D690	–
G	Greenness index	$R554/R677$	Zarco-Tejada et al. (2005)
GM_94a	Gitelson and Merzlyak 1994	$R750/R700$	Gitelson and Merzlyak (1994)
$gNDVI_{[780]}$	Green NDVI	$(R780-R550)/(R780+R550)$	Smith et al. (1995)
GRg	Gitelson ratio green	$(R800/R550)-1$	Gitelson et al. (2003)
Macc01	Maccioni 2001	$(R780-R710)/(R780-R680)$	Maccioni et al. (2001)
MCARI1	Modified chlorophyll absorption 1	$1.2 \times (2.5(R800-R670)-1.3(R800-R550))$	Haboudane et al. (2004)
McM_94	McMurtney	$R700/R670$	McMurtrey et al. (1994)
MND	Modified normalized difference	$(R750-R445)/(R750+R705-2R445)$	Sims and Gamon (2002)
MNDVI1	Modified NDVI	$(R755-R745)/(R755+R745)$	Mutanga and Skidmore (2004)
MNDVI8	Modified NDVI	$(R755-R730)/(R755+R730)$	Mutanga and Skidmore (2004)
MNDVIre	Modified NDVI	$(R750-R705)/(R750+R705-R445)$	Sims and Gamon (2002)
MTCI	MERIS terrestrial chlorophyll index	$(R754 - R709)/(R709 - R681)$	Dash and Curran (2004)
$NDVI_{[800,680]}$	Normalized difference VI [800,680]	$(R800 - R680)/(R800+R680)$	Rouse et al. (1974)
NDVIre	Normalized difference VI – red edge	$(R750 - R705)/(R750+R705)$	Gitelson and Merzlyak (1994)
NPCI	Normalized pigment chlorophyll index	$(R680 - R430)/(R680+R430)$	Peñuelas et al. (1995)
OSAVI	Optimized soil adjusted VI	$1.16 \times (R800 - R670)/(R800 + R670 + 0.16)$	Rondeaux et al. (1996)
PSSRa	Pigment specific simple ratio Chl a	$R800/R680$	Blackburn (1998b)
PSSRb	Pigment specific simple ratio Chl b	$R800/R635$	Blackburn (1998b)
REIP	Red edge inflection point	$(700 + 40 \times ((Rre - R700)/(R740 - R700)))/100$	Guyot and Baret (1988)
REslope1	Derivative reflectance – positive slope	$\sim D710$	Mutanga and Skidmore (2007)
REslope2	Derivative reflectance – negative slope	$\sim D740$	Mutanga and Skidmore (2007)
RMCARI	Revised MCARI	$((R750-R705)-0.2(R750-R550)) \times (R750/R705)$	Wu et al. (2008)
RMCARI/ROSAVI	Ratio of RMCARI/ROSAVI	$RMCARI/ROSAVI$	Wu et al. (2008)
RMSR	Revised MSR	$((R750/R705) - 1)/\text{sqrt}((R750/R705) + 1)$	Wu et al. (2008)
ROSAVI	Revised OSAVI	$1.16 \times (R750 - R705)/(R750 + R705 + 0.16)$	Wu et al. (2008)
Rre	Reflectance at the inflection point	$(R670 + R780)/2$	Guyot and Baret (1988)
RTCARI	Revised Transformed chlorophyll absorption index	$3((R750-R705)-0.2(R750-R550)) \times (R750/R705)$	Wu et al. (2008)
RTCARI/ROSAVI	Ratio of RTCARI/ROSAVI	$RTCARI/ROSAVI$	Wu et al. (2008)
$SIP_{[680]}$	Structure insensitive pigment index [680]	$(R800-R455)/(R800-R680)$	Peñuelas et al. (1995)
$SIP_{[705]}$	Structure insensitive pigment index [705]	$(R800 - R455)/(R800 + R705)$	Peñuelas et al. (1995)
SR	Simple ratio VI	$R800/R670$	Jordan (1969)
$SR_{[750,550]}$	Simple ratio VI [750,550]	$R750/R550$	Gitelson and Merzlyak (1997)
TVI	Triangular VI	$0.5 \times (120(R750 - R550) - 200(R670 - R550))$	Broge and Leblanc (2001)
$VI_{[700]}$	VI – 700nm	$(R700 - R670)/(R700 + R670)$	Gitelson et al. (2002)
VOG1	Vogelmann index	$R740/R720$	Vogelmann et al. (1993)
VOG2	Vogelmann index	$(R734 - R747)/(R715 + R726)$	Vogelmann et al. (1993)
VogD	Vogelmann derivative index	$D715/D705$	Vogelmann et al. (1993)
ZM	Zarco and miller	$R750/R710$	Zarco-Tejada et al. (2001)

A total of 47 published indices were tested in this study (Table 2), in order to assess the most suitable indices for estimating leaf chlorophyll content from broadleaves and needle leaves, both separately and in combination. The most appropriate wavelengths would increase sensitivity to chlorophyll content, whilst reducing effects of other leaf and canopy variables.

At the leaf level, VIs were calculated directly from hyperspectral reflectance data measured using the ASD spectroradiometer. At the canopy level, VIs were derived from interpolated MERIS reflectance data, for the pixel corresponding to the location of the ground-based sampling campaign.

#### 2.4. Leaf and canopy level sensitivity study

The sensitivity study was performed using simulated leaf and canopy reflectance data in order to fix and vary select parameters of interest across a complete range of values and conditions, which are difficult to obtain in measured data. Sensitivity analyses can be 'local', as in this case, where parameters are varied one at a time to determine the effect of individual parameters on model output, or 'global', where all parameters are varied simultaneously

throughout all the parameter space (Fieberg and Jenkins, 2005). It should be noted that these simulations represent modelled scenarios and are not universally valid. The PROSPECT model was used for leaf reflectance simulation because it is a widely accepted model in simulating leaf reflectance of different biochemical components (Jacquemoud and Baret, 1990). Leaf optical properties (reflectance and transmittance) from 400 to 2500 nm are defined in PROSPECT as a function of four parameters: structure parameter (N), chlorophyll ( $a + b$ ) ( $C_{ab}$ ) concentration, dry matter ( $C_m$ ) content and water ( $C_w$ ). To investigate the sensitivity of the VI to chlorophyll content, the chlorophyll content ranged from 10 to 70  $\mu\text{g}/\text{cm}^2$ , while the other parameters were assigned with normal values (Table 3). The selection of parameters values were based on laboratory measurements, inversions conducted at leaf level and published studies (Verrelst et al., 2008; Féret et al., 2008), and varied for simulated broadleaf and needleleaf reflectance.

Canopy reflectance was simulated with the 4-Scale geometrical optical radiative transfer model (Chen and Leblanc, 1997) using the modelled leaf reflectance spectra from PROSPECT. The 4-Scale model simulates the bidirectional reflectance distribution function (BRDF) based on canopy architecture at four scales: (1) tree groups,



**Table 3**  
Fixed and variable leaf parameters used in broadleaf and needleleaf reflectance simulation using the PROSPECT model.

Parameter	Broadleaf	Needleleaf	Unit	Description
N	1.4	2.6	–	Mesophyll structural parameter
Cab	10–70	10–70	$\mu\text{g}/\text{cm}^2$	Chlorophyll content
Cw	0.005	0.001	$\text{g}/\text{cm}^2$	Equivalent water thickness
Cm	0.004	0.035	$\text{g}/\text{cm}^2$	Dry matter content

**Table 4**  
Fixed and variable parameters used in broadleaf and coniferous canopy reflectance simulation using the 4-Scale model.

Parameter	Broadleaf	Coniferous
Leaf reflectance	from PROSPECT model	from PROSPECT model
Solar/viewing geometry	Sza = 30, vza = 0	Sza = 30, vza = 0
LAI	1–10	1–10
Stem height ( $H_a$ )	10	5
Crown height ( $H_b$ )	8	5
Crown radius ( $R$ ) metres	1.25	0.85
Crown shape	Spherical	Cone + cylinder
Tree density (per hectare)	1100	2800
Neyman tree grouping factor	2	4
Element clumping index ( $\Omega E$ )	0.93	0.86
Needle:shoot ratio ( $\gamma E$ )	1	1.4
Element width ( $W_s$ )	0.15	0.04
Understory vegetation and background	Tealeaf willow, lichen, soil, wood	Tealeaf willow, lichen, soil, wood

(2) tree crown geometry, (3) branches, and (4) foliage elements (Chen and Leblanc, 2001). Deciduous crowns are modelled as a spheroid and coniferous crowns as a cone and cylinder, both of variable dimensions. The fixed structural parameters are listed in Table 4, along with LAI which was incremented from 1 to 10 and

the background condition. The background input was from measured reflectance spectra using an ASD Fieldspec ProFR spectroradiometer and weighted according to typical scene fractions observed during field campaigns. The broadleaf and needleleaf reflectance simulated by PROSPECT was used as the input reflectance spectra.

### 3. Results

Fig. 1 shows the differences that exist between measured reflectance spectra for a typical broadleaf (Sugar Maple) and needleleaf (Black Spruce) at the leaf level, and the canopy level from interpolated MERIS data (Section 2.2.2). Spectral differences between species exist due to variations in leaf biochemistry such as chlorophyll content, but also due leaf structure and composition, and at the canopy level due to canopy architecture and background contributions. These confounding variables that affect leaf and canopy spectra demonstrate the difficulty in retrieving leaf chlorophyll over different leaf and canopy structures using reflectance spectra. First derivative spectra have been suggested to correct for variation in leaf surface scattering and variability due to changing illumination and viewing geometries and/or background reflectance (Elvidge and Chen, 1995; Vogelmann et al., 1993). First derivative spectra were calculated as the slope of the

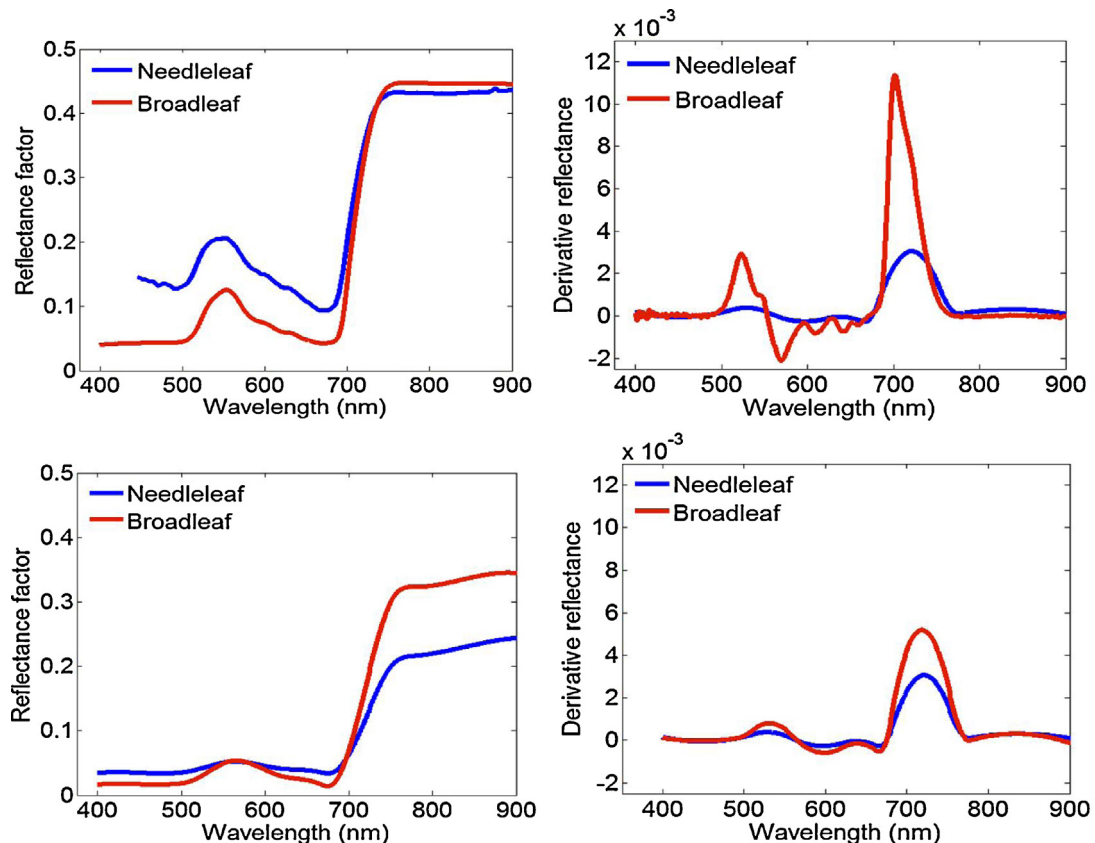


**Fig. 1.** Reflectance and first derivative spectra for broadleaf and needle leaves at the leaf (two top figures) and canopy scale (two bottom figures).

reflectance spectra (Richardson et al., 2003), shown alongside original reflectance spectra for broadleaf and needleleaf samples.

### 3.1. Chlorophyll content and vegetation indices at the leaf level

To first assess the relationship between VIs and chlorophyll content for both species without the influence of confounding canopy variables, relationships are first explored the leaf level. VIs calculated using leaf reflectance factors are regressed against leaf chlorophyll content for each leaf type individually and for both species combined. Fig. 2 shows the index having the strongest relationship with leaf chlorophyll (see Appendix I) in each case (broadleaf, needleleaf and combined leaf types).

The broadleaves show a very strong relationship with leaf chlorophyll, with a regression coefficient of  $R^2 = 0.80$ . For needleleaves, the relationship is weaker ( $R^2 = 0.61$ ), displaying greater scatter around the regression line. When both leaf types are combined, the relationship is strong ( $R^2 = 0.72$ ) despite the differences in the internal structural composition of both leaf types. However, there does appear to be an underestimation of MTCI values for higher needleleaf chlorophyll contents and a potential lack of sensitivity to changes in needleleaf chlorophyll content.

The highest ranking broadleaf indices (Appendix I) are focussed on reflectance factors or derivative reflectance from wavelengths on the red-edge, which is the sharp transition from low reflectance at an inflection point around 680 nm to high reflectance at around 750 nm. In contrast, the majority of the best performing indices for needleleaf and combined results are modified simple ratios, including a structural component or index band (750–850 nm) and a chlorophyll absorption band (680 nm). The top three

performing vegetation indices for needleleaf samples show weaker relationships with chlorophyll content ( $R^2 = 0.61$ – $0.59$ ). Notably, despite MNDVI8 featuring as the top performing index for both broadleaf and needleleaf samples individually, the results for the combined dataset rank slightly lower at eighth in the table, where  $R^2 = 0.68$  and RMSE =  $6.39 \mu\text{g}/\text{cm}^2$  (Appendix I).

### 3.2. Chlorophyll content and vegetation indices at the canopy level

Many VIs have been developed at the leaf level and applied to canopy reflectance. However, the influence of other canopy variables such as LAI and canopy architecture, non-photosynthetic elements and background contributions from understory vegetation and soil all contribute to canopy reflectance. A number of VIs have also been developed at the canopy scale, such as RMCARI, MTCI, OSAVI, RTCARI and ROSAVI (Dash and Curran, 2004; Haboudane et al., 2002, 2004; Rondeaux et al., 1996; Wu et al., 2008). Fig. 3 shows the best case relationship between VIs calculated using MERIS (300 m) canopy reflectance and leaf chlorophyll content for individual leaf types and combined leaf types.

Broadleaf chlorophyll content displays an extremely strong relationship with the Macc01 index ( $R^2 = 0.98$ ), derived from MERIS satellite data. Despite the presence of perturbing canopy variables and a greater background contribution due to lower LAI values and increased foliage clumping, the derivative reflectance at a single wavelength (690 nm) shows a very good relationship with needleleaf chlorophyll content at the canopy level ( $D_{[\text{red}]}$ ;  $R^2 = 0.71$ ). The combined leaf types also display a strong relationship ( $R^2 = 0.78$ ) with the Datt Derivative index, despite differences in leaf and canopy structure.

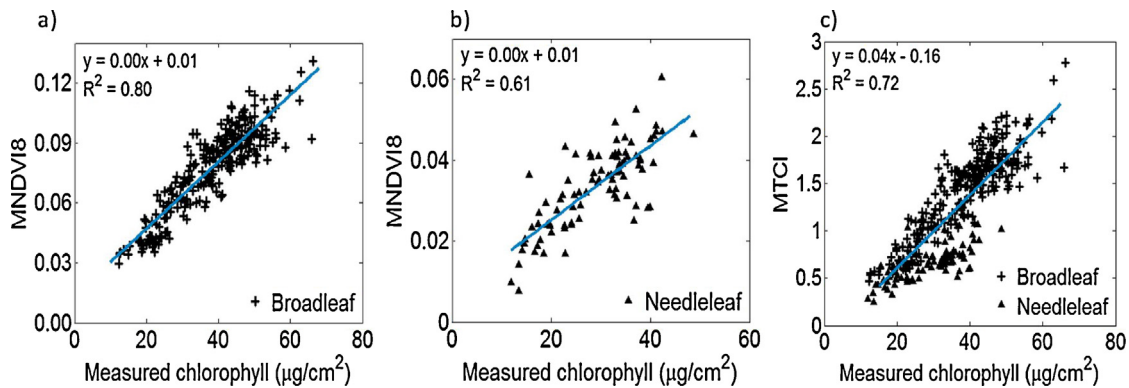


Fig. 2. Best performing VIs at the leaf level for (a) broadleaf sites (MNDVI8;  $R^2 = 0.80$ ,  $p < 0.001$ ); (b) needle sites (MNDVI8;  $R^2 = 0.61$ ,  $p < 0.001$ ); and (c) all sites (MTCI;  $R^2 = 0.72$ ,  $p < 0.001$ ).

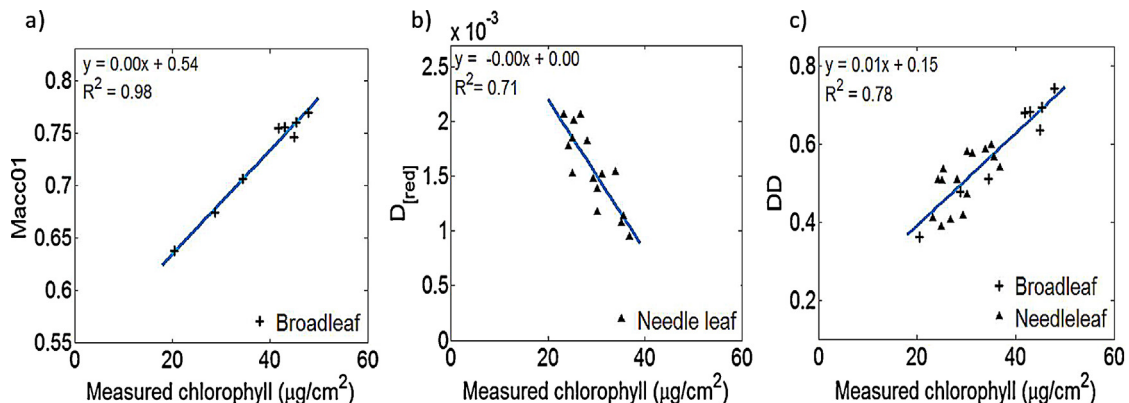


Fig. 3. Best performing VIs at the canopy level for (a) broadleaf sites (Macc01;  $R^2 = 0.98$ ); (b) needle sites ( $D_{[\text{red}]}$ ;  $R^2 = 0.71$ ); and (c) all sites (DD;  $R^2 = 0.78$ ).

In addition to  $D_{[red]}$ , other derivative indices (DD, VogD) also feature highly in Appendix 1 for needleleaf canopy level VIs, supporting previous findings that they have a reduced sensitivity to variations in canopy structure and background (Demetriades-Shah et al., 1990). RTCARI (needleleaf canopy;  $R^2 = 0.69$ ) has also been shown to be suitable to canopies with large background effects (Zarco-Tejada et al., 2004). The best performing VIs for canopy level broadleaf (Macc01) and combined leaf types (Datt Derivative) show a focus on wavelengths along the red-edge, also echoing findings at the leaf level (Appendix 1). Most of the top performing broadleaf indices at the canopy level (Appendix 1) are red-edge based, with variations in the index wavelength (e.g. R850, R780, R754 nm) used to account for differences in leaf structure. Le Maire et al. (2004) also found the red-edge Datt99 index gave the best results when tested with experimental and simulated data. Interestingly, the top VI for combined leaf types incorporated both derivative reflectance and red-edge wavelengths (DD; D754)/D704).

### 3.3. Sensitivity analysis at the leaf level

In order to investigate further the results found on measured data, a sensitivity analysis was conducted to more thoroughly assess the capacity of the VIs to represent chlorophyll content under a range of different confounding variables. The VIs that are most suitable for chlorophyll estimation will show a linearity with increasing chlorophyll content, which will avoid saturation and

low sensitivity at high chlorophyll content and be insensitive to changing canopy variables.

#### 3.3.1. Leaf level

The simulated results for broadleaf, needleleaf and combined leaf types are shown in Fig. 4 for top-performing and selected indices. The best performing MNDVI8 index for broadleaves also demonstrates a strong linearity for simulated results. In comparison the McM94 index displays a strongly curvilinear response after approximately  $40 \mu\text{g}/\text{cm}^2$ , accounting for the reduced performance in the empirical dataset. Interestingly, the two REslope derivative indices (D710 and D740) show very different results, revealing the importance of the wavelength position along the red-edge, which is well-reported for its sensitivity to chlorophyll (Curran et al., 1991). The linearity in response from the red-edge shoulder at 740 nm supports the importance of this location, with many of the top ten indices for the broadleaf dataset being focused on this region (Appendix 1).

The MNDVI8 and REslope2 indices show a very strong linearity in comparison to indices focussed on wavelengths closer to the red absorption band and base of the red-edge. The top-performing index in the measured dataset for both leaf types combined was MTCI ( $R^2 = 0.71$ ), however, Fig. 4 reveals a separation after approximately  $40 \mu\text{g}/\text{cm}^2$ , with broadleaf MTCI being higher than corresponding needleleaf values for the same chlorophyll content. The REslope2 index shows a dependency on leaf structure, suggesting that although the red-edge shoulder appears to be

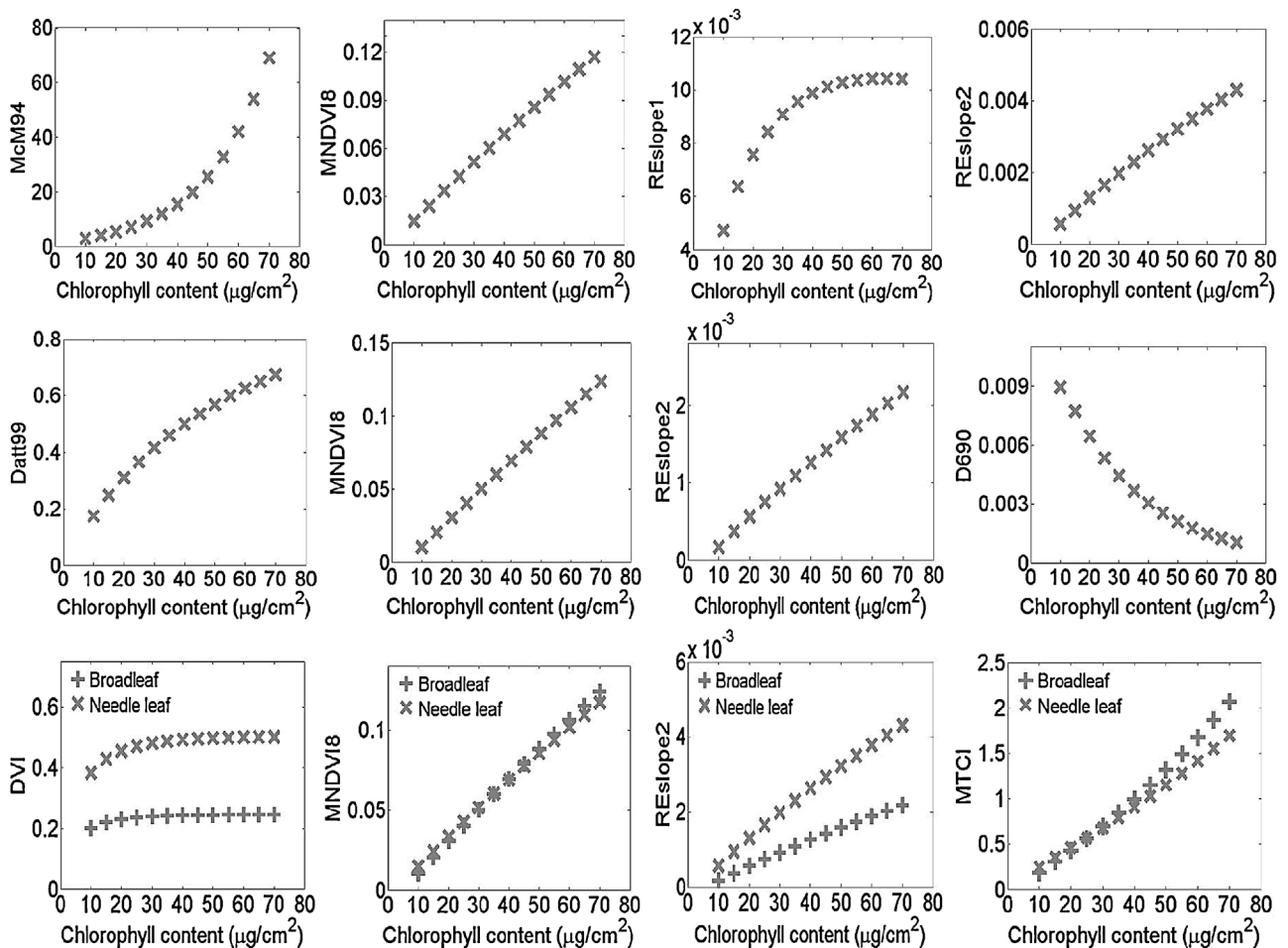


Fig. 4. The relationship between chlorophyll content and VIs calculated from simulated leaf reflectance spectra, where the first row = broadleaf data, second row = needleleaf data, third row = combined leaf types.

sensitive to high chlorophyll content, the lack of an additional band to normalize the value at D740 nm, reduces its applicability over different leaf types. This is supported by the poor performance of DVI (=800–670 nm), which shows little sensitivity to chlorophyll content, saturating at approximately  $30 \mu\text{g}/\text{cm}^2$  and a large difference based on leaf type. Conversely, MNDVI8 again shows very consistent results for both leaf types, indicating that leaf structure plays little influence in its ability to retrieve chlorophyll content at the leaf level.

### 3.3.2. Canopy level

The performance of indices at the canopy scale may differ from the leaf scale due to the presence of confounding variables such as leaf area index and background composition. Vegetation indices were calculated from modelled canopy spectra, using the 4-Scale geometrical-optical radiative transfer model (Chen and Leblanc, 1997) in order to assess the relative contribution of these factors to VI sensitivity to leaf chlorophyll content. Fig. 5 shows the top-performing and interesting VIs for broadleaf and needleleaf datasets.

The top-performing canopy broadleaf index (Datt99) shows a slightly non-linear response at higher chlorophyll content, in comparison to MNDVI8. Both indices for broadleaf show little sensitivity to different LAI values, with only LAI = 2 displaying largely different results. As expected, the needleleaf canopy results show slightly more variability, with the RESlope2 index revealing a strong sensitivity to LAI changes. The MDNV18 index performed strongly on simulated leaf level data (Fig. 4) and demonstrates a linear relationship with Chlorophyll and relatively little sensitivity to changes in LAI, where LAI = >4.

The background composition was varied within 4-Scale for the modelled canopy results in order to test the VIs responses to different spectra. The LAI values were set at LAI = 2, in order to be able to detect any differences, in background particularly for broadleaf canopies. The four background types selected were

tealeaf willow, lichen, soil and wood, in order to provide a range of spectral characteristics.

The response of the VIs shown in Fig. 6 to the influence of background composition on the relationship with chlorophyll content at low LAI values is considerable. The TCARI/OSAVI has been reported to reduce the influence of background effects, however, the simulated results still show large differences.

### 3.3.3. Wavelength regions of maximum chlorophyll sensitivity

The difference between modelled leaf and canopy reflectance spectra for leaf chlorophyll contents of  $10 \mu\text{g}/\text{cm}^2$  and  $70 \mu\text{g}/\text{cm}^2$  was calculated, in order to investigate the wavelength regions of maximum sensitivity to chlorophyll differences (Fig. 7). The LAI was fixed at LAI = 4 and the background vegetation tealeaf willow; therefore giving an indication of the sensitivity response of medium/dense canopies. At the leaf scale the two regions demonstrating high sensitivity to chlorophyll differences was in the green and red-edge, with maximum values occurring at 559 nm and 704 nm, and 560 nm and 699 nm, for broadleaf and needle respectively.

For the canopy level, the green wavelengths were less sensitive to chlorophyll differences, likely due to the confounding influence of LAI. Red wavelengths were also less important and the maximum positions of difference were the same as the leaf scale for green wavelengths and 715 and 712 nm along the red-edge for broadleaf and needle respectively.

## 4. Discussion

### 4.1. Chlorophyll vegetation indices and vegetation type

In order to apply VIs across broad spatial extents, without extensive ground calibration and across areas with heterogeneous canopies, such as in the mixed forests typical of the southern Boreal regions, it is crucial that the VI is applicable at the canopy

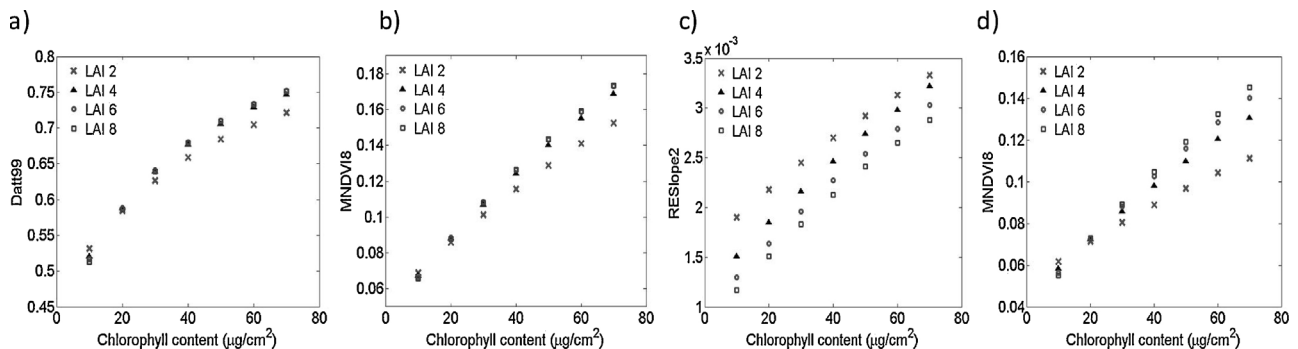


Fig. 5. The influence of LAI on the relationship between VIs and leaf chlorophyll for (a) and (b) broadleaf; (c) and (d) needleleaf.

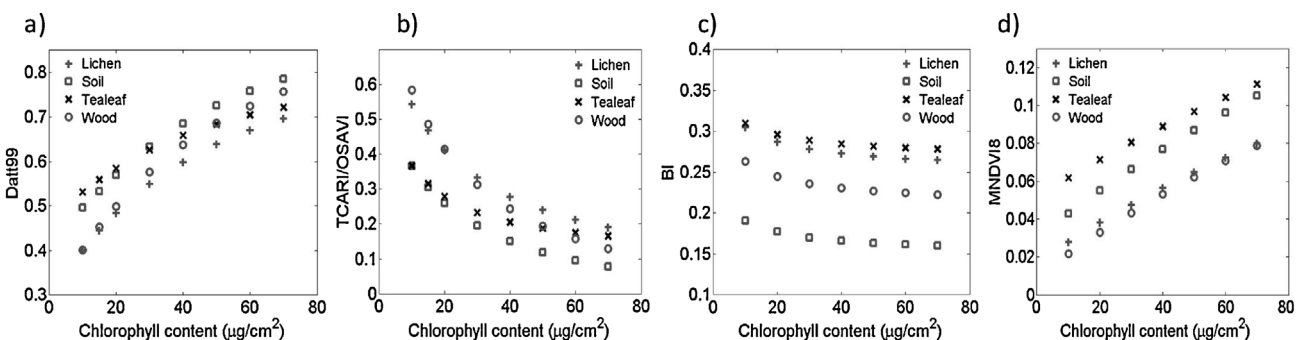
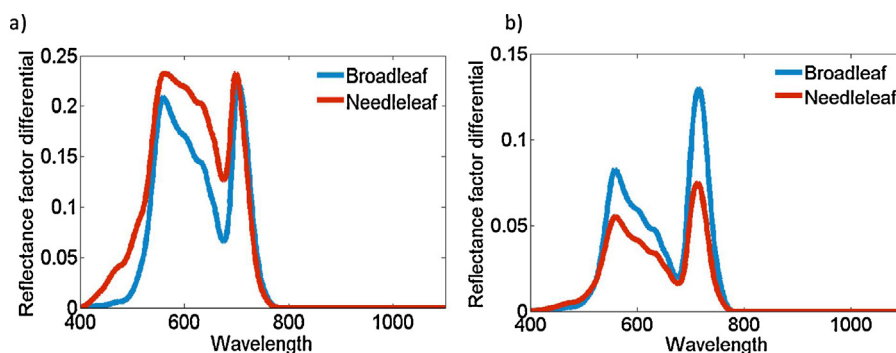


Fig. 6. The influence of background characteristics on the relationship between VIs and leaf chlorophyll for (a) and (b) broadleaf; (c) and (d) needleleaf (LAI = 2).





**Fig. 7.** Wavelength regions of maximum difference between modelled (a) leaf and (b) canopy reflectance spectra (LAI = 4, background = tealeaf willow), for Cab = 10  $\mu\text{g}/\text{cm}^2$  and 70  $\mu\text{g}/\text{cm}^2$ .

level across different leaf functional types. The majority of published vegetation indices have been developed and tested on broadleaf species, with considerably less research focussed on needleleaf species. The broadleaf sites performed extremely well at leaf and canopy levels, in accordance with previously published relationships with leaf chlorophyll content (Haboudane et al., 2008). The relationship between needleleaf VIs and leaf chlorophyll were weaker ( $R^2 = 0.61$ ), even at the leaf level, without the influence of canopy variables. Whilst, the simulated results showed strong results from modelled needleleaf reflectance, the dry matter, internal structure and water content parameters were fixed, which would vary in actual leaf samples. Finite leaf width and variable thickness of conifer needles increases the complexity in the relationship between reflectance from spectra and chlorophyll content (Zarco-Tejada et al., 2004; Zhang et al., 2008a). The weaker results for the measured dataset could also be due to error in chlorophyll laboratory or leaf reflectance measurements. The measurement of the optical properties of needle leaves is not trivial, which may partially account for the relatively small number of needleleaf studies, compared to broadleaf applications (Jacquemoud and Ustin, 2001). Disparities could also occur due to a heterogeneous distribution of pigments in leaf tissue (Sims and Gamon, 2002).

Nonetheless, the poor performance of VIs with measured needleleaf chlorophyll content suggests that further research is required to better represent differences in pigment content and reduce the sensitivity of the VI to leaf structure, leaf thickness and water content for needleleaf species (Main et al., 2011). Serrano (2008) also observed a decrease in R800 with corresponding increases in leaf thickness in *Cistus ladanifer* and *Nerium oleander* species, which was attributed to greater palisade to spongy parenchyma thickness ratio. Reduced NIR scattering from spongy mesophyll cells, may consequently lead to lower NIR reflectance values from the adaxial surface (Serrano, 2008) and lower ND and SR index values. The MNDVI8 index, focussed on the red-edge shoulder showed considerable potential in removing the influence of leaf structure within the sensitivity study, displaying only negligible differences between simulated MDNVI8 and leaf chlorophyll for both leaf types across all simulated chlorophyll contents.

#### 4.2. Scale specific relationships at the leaf and canopy level

Many VIs have been developed on leaf level samples, which then are difficult to apply to the canopy level due to a greater complexity in the canopy scene. For broadleaf species, a large number of VIs do appear in the top rankings for both leaf and canopy levels, (e.g. Datt99, Macc01, ZM and VOG1/VOG2) although the actual values differ. The close correspondence is because for

uniform, closed canopies, the vegetation stand effectively behaves like a 'big leaf' (Gamon et al., 2010) and other perturbing variables, such as background contributions are low. The sensitivity study demonstrated the profound effects that different background variables have on VIs, with even the consistently top-performing indices (e.g. MNDVI8, Datt99) showing large dependence on background properties. The influence of increasing LAI (Fig. 5) had little influence on the top-performing red-edge VIs for broadleaf data where LAI  $\geq 4$ . The needleleaf canopy data showed more variability, particularly in the case of MNDVI8 after chlorophyll content exceeded 40  $\mu\text{g}/\text{cm}^2$ , although variations were still relatively small, depending on the selected VI.

#### 4.3. Type of spectral indices

At the canopy level, the highest ranking indices for combined leaf types was a simple ratio of  $\sim R750$  to compensate for internal leaf scattering (Coops and Stone, 2005) divided by a chlorophyll sensitive band between R700 to R720 (Appendix I). Research has shown that bands along the red-edge region are strongly related to chlorophyll content (Curran et al., 1991). A broadening of the absorption feature centred around 680 nm, due to increased chlorophyll content, shifts the point of maximum slope (Dawson and Curran, 1998). Interestingly, this dependence on wavelengths along the red-edge was less apparent for the needleleaf canopy. The preponderance to 'off-centre' chlorophyll bands also supports previous findings of chlorophyll absorption wavelengths (660–680 nm) to be poor indicators of chlorophyll content, due to ready saturation even at low chlorophyll content (Wu et al., 2008; Daughtry et al., 2000). Indices including 'off-centre' wavelengths (690–730 nm), are suggested to have greater sensitivity to subtler changes in chlorophyll content (Main et al., 2011). Whilst the preference for off-centre chlorophyll bands existed for the combined canopy leaf types, when tested individually, and for the combined leaf level dataset approximately half of the top VIs contained either R670 or R680 (Tables 3 and 4).

Reflectance derivatives at single wavelengths and within derivative vegetation indices have been reported to be related to chlorophyll content at leaf and canopy scales (Main et al., 2011; Vogelmann et al., 1993). Interestingly, results from this study found that whilst derivatives failed to feature highly in relationships at the leaf level, they were closely related to leaf chlorophyll at the canopy level (Appendix I). Conversely, several of the worst performing indices for combined leaf types at the canopy level contained wavelengths exclusively below 700 nm (BGI, TCARI, PRI;  $R^2 = <0.04$  and RMSE =  $<7.44 \mu\text{g}/\text{cm}^2$ ). However, needle leaves show a greater propensity for VIs comprising exclusively visible wavelengths (e.g. CUR, TCARI, G), particularly at the green peak ( $\sim 550$  nm) and chlorophyll absorption feature.

## 5. Conclusion

Efforts to estimate leaf chlorophyll content from empirically-driven vegetation indices have focused on broadleaf species, both in terms of development and validation. This research has tested the performance of a large number of vegetation indices across leaf types at both the leaf and canopy scale, in order to (a) assess the influences of leaf structure and canopy structure on the relationship between VIs and leaf chlorophyll content, and (b) investigate the type of indices or preferred combinations of wavelengths that are suitable for different vegetation functional types and observational scales. When the leaf types are considered separately, the broadleaf samples exhibit extremely strong relationships between spectral indices and leaf chlorophyll content, and presented strong results at leaf and canopy scales. This study found that at the canopy scale the best performing indices were (a) broadleaf canopies: Macc01 ( $R^2 = 0.98$ ; RSME =  $1.33 \mu\text{g}/\text{cm}^2$ ); (b) needleleaf canopies:  $D_{[\text{red}]}$  ( $R^2 = 0.71$ ; RSME =  $2.32 \mu\text{g}/\text{cm}^2$ ) and (c) combined dataset canopies: DD ( $R^2 = 0.78$ ; RSME =  $3.56 \mu\text{g}/\text{cm}^2$ ). Through the use of a large simulated dataset generated using leaf and canopy radiative transfer models, the profound influence of background composition was highlighted. However, variations

in canopy structure after LAI = 4, seemed to have little influence on the best performing indices. At the leaf level, the top index using simulated data was found to be MNDV18, derived from the red-edge shoulder, and shows little sensitivity to differences in modelled leaf structure. This was confirmed by the measured combined leaf type dataset (Appendix I).

The scope of monitoring leaf chlorophyll content across large spatial extents and across small time-frames using remote sensing techniques is important for a range of ecological applications. However, these results suggest that care should be taken in selecting and applying a spectral index, according to leaf type, observational scale, LAI and background variables. Furthermore, it suggests that further research is required to empirically account for background variables in terms of developing a universal VI, and that it may be preferable to design ecosystem specific indices.

## Acknowledgements

This research was funded by a grant from the Natural Sciences and Engineering Research Council, Canada. The European Space Agency provided the MERIS FR L2 data for this study.

## Appendix I

The relationship between leaf chlorophyll and all tested spectral indices for each type individually and combined, at leaf and canopy scales (RMSE = root mean square error).

Broadleaf			Needleleaf			All leaf level			Broadleaf canopy			Needleleaf canopy			All canopy level		
Index	$R^2$	RMSE	Index	$R^2$	RMSE	Index	$R^2$	RMSE	Index	$R^2$	RMSE	Index	$R^2$	RMSE	Index	$R^2$	RMSE
MNDV18	0.80	4.97	MNDV18	0.61	5.32	MTCI	0.72	6.03	Macc01	0.98	1.33	$D_{[\text{red}]}$	0.71	2.32	DD	0.78	3.56
REslope2	0.79	5.01	Datt99	0.60	5.42	Datt99	0.71	6.13	MTCI	0.96	1.73	RTCARI	0.69	2.39	MTCI	0.74	3.90
RMCARI/ ROSAVI	0.79	5.04	Macc01	0.59	5.48	Macc01	0.71	6.13	VogD	0.96	1.75	BI	0.62	2.65	REIP	0.74	3.90
RMSR	0.79	5.02	VOG1	0.58	5.53	MND	0.70	6.18	DD	0.95	1.96	Rre	0.58	2.81	MNDV11	0.71	4.10
RMCARI	0.79	5.05	REIP	0.57	5.62	VOG1	0.69	6.31	MNDV11	0.95	2.04	RTCARI/ ROSAVI	0.55	2.91	Macc01	0.71	4.15
MND	0.79	5.02	ZM	0.56	5.65	MNDV18	0.68	6.36	REIP	0.94	2.21	MTCI	0.43	3.25	VOG2	0.7	4.17
ZM	0.79	5.04	NDVire	0.56	5.67	RMCARI_ ROSAVI	0.68	6.38	Datt99	0.93	2.31	VogD	0.43	3.27	VogD	0.7	4.21
VOG2	0.79	5.07	ROSAVI	0.56	5.69	ZM	0.68	6.40	MNDV18	0.91	2.63	DD	0.42	3.30	Datt99	0.7	4.21
MNDVire	0.79	5.05	RMSR	0.55	5.72	VOG2	0.68	6.42	VOG2	0.89	2.94	Datt99	0.41	3.32	RTCARI/ ROSAVI	0.69	4.23
VOG1	0.79	5.07	MNDVire	0.55	5.75	RMCARI	0.68	6.44	MNDVire	0.88	3.12	Macc01	0.40	3.34	ZM	0.68	4.31
ROSAVI	0.79	5.08	MTCI	0.55	5.75	MNDVire	0.66	6.55	MND	0.88	3.13	REslope1	0.39	3.38	MNDV18	0.68	4.34
Datt99	0.79	5.10	VOG2	0.55	5.76	MNDV11	0.65	6.66	VOG1	0.85	3.46	VOG2	0.38	3.41	VOG1	0.67	4.36
NDVire	0.79	5.09	CI	0.53	5.84	RMSR	0.65	6.67	ZM	0.81	3.89	REIP	0.37	3.42	MNDVire	0.64	4.56
Macc01	0.78	5.11	$g\text{NDVI}_{[780]}$	0.52	5.89	NDVire	0.63	6.87	RMSR	0.75	4.51	ZM	0.37	3.42	RMSR	0.64	4.62
GM_94a	0.78	5.13	GM_94a	0.51	5.96	ROSAVI	0.63	6.87	NDVire	0.74	4.54	VOG1	0.37	3.43	MND	0.63	4.63
MTCI	0.78	5.17	CTR	0.50	6.02	GM_94a	0.63	6.90	RTCARI/ ROSAVI	0.69	4.98	MND	0.37	3.43	RTCARI	0.63	4.64
SIPI <sub>[705]</sub>	0.77	5.25	GRg	0.49	6.07	REslope2	0.61	7.04	GM_94a	0.63	5.43	G	0.37	3.43	GM_94a	0.63	4.65
VogD	0.76	5.35	RMCARI	0.49	6.10	REIP	0.59	7.24	RTCARI	0.58	5.83	MNDV18	0.36	3.44	NDVire	0.59	4.91
RTCARI/ ROSAVI	0.75	5.44	$SR_{[750,550]}$	0.49	6.12	GRg	0.59	7.23	CTR	0.49	6.43	MNDV11	0.36	3.45	CTR	0.46	5.61
REIP	0.75	5.53	MND	0.45	6.33	$SR_{[750,550]}$	0.58	7.31	BGI	0.47	6.51	MNDVire	0.36	3.45	PSSRb	0.42	5.84
MNDV11	0.74	5.69	RTCARI	0.39	6.66	RTCARI_ ROSAVI	0.55	7.59	$D_{[\text{red}]}$	0.45	6.66	GM_94a	0.36	3.46	SIPI <sub>[705]</sub>	0.40	5.92
GRg	0.74	5.61	RTCARI/ ROSAVI	0.35	6.88	$D_{[\text{red}]}$	0.54	7.62	SIPI <sub>[680]</sub>	0.41	6.88	RMSR	0.36	3.47	GRg	0.4	5.94
VI <sub>[700]</sub>	0.74	5.65	$D_{[\text{red}]}$	0.33	7.01	$g\text{NDVI}_{[780]}$	0.52	7.88	NPCI	0.38	7.04	NDVire	0.34	3.51	NPCI	0.38	6.02
$SR_{[750,550]}$	0.73	5.72	MNDV11	0.32	7.03	CUR	0.49	8.08	McM_94	0.33	7.33	DVI	0.31	3.59	$SR_{[750,550]}$	0.37	6.06
CTR	0.73	5.75	PSSRb	0.32	7.06	CI	0.49	8.13	VI <sub>[700]</sub>	0.29	7.54	TVI	0.31	3.60	RMCARI	0.37	6.08
BGI	0.73	5.82	RMCARI/ ROSAVI	0.31	7.11	PSSRb	0.44	8.47	CUR	0.20	8.00	MCARI1	0.30	3.61	$g\text{NDVI}_{[780]}$	0.36	6.09
McM_94	0.72	5.87	SIPI <sub>[705]</sub>	0.29	7.2	SIPI <sub>[705]</sub>	0.44	8.53	RMCARI	0.18	8.10	PSSRb	0.30	3.61	SIPI <sub>[680]</sub>	0.36	6.13
$g\text{NDVI}_{[780]}$	0.72	5.87	REslope1	0.18	7.73	CTR	0.44	8.53	G	0.18	8.11	SR	0.30	3.61	CI	0.36	6.14
$D_{[\text{red}]}$	0.71	5.93	BI	0.17	7.76	G	0.43	8.61	ROSAVI	0.17	8.16	PSSRa	0.30	3.61	RMCARI/ ROSAVI	0.35	6.16
CI	0.70	6.02	REslope2	0.14	7.91	VogD	0.42	8.62	SIPI <sub>[705]</sub>	0.17	8.17	CTR	0.29	3.63	ROSAVI	0.34	6.23

## Appendix I (Continued)

Broadleaf			Needleleaf			All leaf level			Broadleaf canopy			Needleleaf canopy			All canopy level		
Index	R <sup>2</sup>	RMSE	Index	R <sup>2</sup>	RMSE	Index	R <sup>2</sup>	RMSE	Index	R <sup>2</sup>	RMSE	Index	R <sup>2</sup>	RMSE	Index	R <sup>2</sup>	RMSE
DD	0.63	6.86	OSAVI	0.11	8.08	RESlope1	0.39	8.92	RMCARI/ ROSAVI	0.16	8.19	NPCI	0.26	3.72	NDVI <sub>[800,680]</sub>	0.31	6.33
PSSRb	0.62	6.75	CUR	0.10	8.10	DVI	0.30	9.52	CI	0.12	8.4	SIP <sub>[705]</sub>	0.25	3.73	PSSRa	0.26	6.58
G	0.61	6.91	NDVI <sub>[800,680]</sub>	0.09	8.13	McM <sub>94</sub>	0.30	9.51	gNDVI <sub>[780]</sub>	0.11	8.42	NDVI <sub>[800,680]</sub>	0.25	3.75	RESlope2	0.25	6.61
RESlope1	0.52	7.77	SR	0.06	8.28	BGI	0.28	9.65	GRg	0.11	8.46	SIP <sub>[680]</sub>	0.24	3.76	SR	0.25	6.63
CUR	0.50	7.73	PSSRa	0.06	8.29	VI <sub>[700]</sub>	0.25	9.81	PSSRb	0.10	8.50	GRg	0.2	3.86	OSAVI	0.15	7.06
DVI	0.40	8.7	G	0.05	8.31	BI	0.23	9.99	RESlope2	0.09	8.53	SR <sub>[750,550]</sub>	0.2	3.87	CUR	0.15	7.06
Rre	0.37	8.89	DVI	0.05	8.34	PSSRa	0.23	10.01	SR <sub>[750,550]</sub>	0.07	8.62	gNDVI <sub>[780]</sub>	0.18	3.91	DVI	0.13	7.15
OSAVI	0.36	8.98	MCARI1	0.03	8.40	OSAVI	0.22	10.06	RESlope1	0.02	8.86	CI	0.18	3.92	MCARI1	0.11	7.20
NDVI <sub>[800,680]</sub>	0.21	9.95	SIP <sub>[680]</sub>	0.03	8.40	SR	0.21	10.11	OSAVI	0.01	8.91	McM <sub>94</sub>	0.17	3.94	VI <sub>[700]</sub>	0.11	7.22
MCARI1	0.21	9.83	Rre	0.02	8.44	DD	0.21	10.16	SR	0.01	8.92	VI <sub>[700]</sub>	0.16	3.96	TVI	0.10	7.27
RTCARI	0.21	9.96	NPCI	0.02	8.47	NDVI <sub>[800,680]</sub>	0.19	10.25	PSSRa	0.00	8.93	CUR	0.14	4.00	RESlope1	0.07	7.39
PSSRa	0.21	9.98	DD	0.01	8.48	MCARI1	0.10	10.77	TVI	0.00	8.94	RESlope2	0.07	4.17	G	0.06	7.40
SR	0.20	10.00	McM <sub>94</sub>	0.01	8.49	SIP <sub>[680]</sub>	0.02	11.28	DVI	0.00	8.95	OSAVI	0.05	4.21	Rre	0.06	7.43
SIP <sub>[680]</sub>	0.18	10.14	VI <sub>[700]</sub>	0.01	8.50	RTCARI	0.02	11.31	Rre	0.00	8.95	BGI	0.02	4.28	McM <sub>94</sub>	0.04	7.48
BI	0.18	10.00	TVI	0.01	8.51	TVI	0.00	11.37	MCARI1	0.00	8.95	ROSAVI	0.01	4.30	BI	0.03	7.52
NPCI	0.15	10.35	VogD	0.01	8.52	Rre	0.00	11.38	BI	0.00	8.95	RMCARI	0.00	4.31	D <sub>[red]</sub>	0.02	7.57
TVI	0.10	10.59	BGI	0.00	8.53	NPCI	0.00	11.4	NDVI <sub>[800,680]</sub>	0.00	8.95	RMCARI/ROSAVI	0.00	4.32	BGI	0.00	7.64

## References

- Blackburn, G.A., 1998. Quantifying chlorophylls and carotenoids at leaf and canopy scales: An evaluation of some hyperspectral approaches. *Remote Sensing of Environment* 66, 273–285.
- Blackburn, G.A., 1998b. Spectral indices for estimating photosynthetic pigment concentrations: A test using senescent tree leaves. *International Journal of Remote Sensing* 19, 657–675.
- Blackburn, G.A., 2006. Hyperspectral remote sensing of plant pigments. *Journal of Experimental Botany* 58 (4), 855–867.
- Broge, N.H., Leblanc, E., 2001. Comparing prediction power and stability of broadband and hyperspectral vegetation indices for estimation of green leaf area index and canopy chlorophyll density. *Remote Sensing of Environment* 76 (2), 156–172.
- Canisius, F., Fernandes, R., 2012. Evaluation of the information content of Medium Resolution Imaging Spectrometer (MERIS) data for regional leaf area index assessment. *Remote Sensing of Environment* 119, 301–314.
- Canisius, F., Fernandes, R., Chen, J.M., 2010. Comparison and evaluation of Medium Resolution Imaging Spectrometer leaf area index products across a range of land use. *Remote Sensing of Environment* 114, 950–960.
- Carter, G.A., 1994. Ratios of leaf reflectances in narrow wavebands as indicators of plant stress. *International Journal of Remote Sensing* 15 (3), 679–703.
- Caspersen, J.P., Sapruff, M., 2005. Seedling recruitment in a northern temperate forest: the relative importance of supply and establishment limitation. *Canadian Journal of Forest Research* 35, 978–989.
- Chen, J.M., Cihlar, J., 1995. Plant canopy gap size analysis theory for improving optical measurements of leaf area index. *Applied Optics* 34, 6211–6222.
- Chen, J.M., Leblanc, S., 1997. A 4-Scale bidirectional reflection model based on canopy architecture. *IEEE Transactions on Geoscience and Remote Sensing* 35, 1316–1337.
- Chen, J.M., Leblanc, S.G., 2001. Multiple-scattering scheme useful for hyperspectral geometrical optical modelling. *IEEE Transactions on Geoscience and Remote Sensing* 39 (5), 1061–1071.
- Chen, J.M., Rich, P.M., Gower, T.S., Norman, J.M., Plummer, S., 1997. Leaf area index of boreal forests: theory, techniques and measurements. *Journal of Geophysical Research* 102 (29), 429–529, 444.
- Coops, N.C., Stone, C., 2005. Use of a radiative transfer model to examine variation in reflectance spectra due to damaged *Pinus radiata* foliage. *Australian Journal of Botany* 53, 417–429.
- Croft, H., Chen, J.M., Zhang, Y., Simic, A., 2013. Modelling leaf chlorophyll content in broadleaf and needle canopies from ground, CASI, Landsat TM 5 and MERIS reflectance data. *Remote Sensing of Environment* 133, 128–140.
- Curran, P.J., Dungan, J.L., Macler, B.A., Plummer, S.E., 1991. The effect of a red leaf pigment on the relationship between red edge and chlorophyll concentration. *Remote Sensing of Environment* 35, 69–76.
- Dash, J., Curran, P.J., 2004. The MERIS terrestrial chlorophyll index. *International Journal of Remote Sensing* 25 (23), 5403–5413.
- Datt, B., 1999. Visible/near infrared reflectance and chlorophyll content in Eucalyptus leaves. *International Journal of Remote Sensing* 20, 2741–2759.
- Daughtry, C.S.T., Walthall, C.L., Kim, M.S., de Colstoun, E.B., McMurtrey, J.E., 2000. Estimating corn leaf chlorophyll concentration from leaf and canopy reflectance. *Remote Sensing of Environment* 74, 229–239.
- Dawson, T.P., Curran, P.J., 1998. A new technique for interpolating the reflectance red edge position. *International Journal of Remote Sensing* 19, 2133–2139.
- Demarez, V., Gastellu-Etchegorry, J.P., 2000. A modeling approach for studying forest chlorophyll content. *Remote Sensing of Environment* 71, 226–238.
- Demetriades-Shah, T.H., Steven, M.D., Clark, J.A., 1990. High resolution derivative spectra in remote sensing. *Remote Sensing of Environment* 33, 55–64.
- Elvidge, C.D., Chen, Z., 1995. Comparison of broad-band and narrow-band red and near-infrared vegetation indices. *Remote Sensing of Environment* 54, 38–48.
- Féret, J.B., François, C., Asner, G.P., Gitelson, A.A., Martin, R.E., Bidol, L.P.R., Ustin, S.L., le Marie, G., Jacquemoud, S., 2008. PROSPECT-4 and 5: advances in the leaf optical properties model separating photosynthetic pigments. *Remote Sensing of Environment* 112 (6), 3030–3043.
- Fieberg, J., Jenkins, K.J., 2005. Assessing uncertainty in ecological systems using global sensitivity analyses: a case example of simulated wolf reintroduction effects on elk. *Ecological Modelling* 187 (2–3), 259–280.
- Filella, I., Serrano, L., Serra, J., Penuelas, J., 1995. Evaluating wheat nitrogen status with canopy reflectance indices and discriminant analysis. *Crop Science* 35, 1400–1405.
- Gamon, J.A., Surfus, J.S., 1999. Assessing leaf pigment content and activity with a reflectometer. *New Phytologist* 143, 105–117.
- Gamon, J.A., Coburn, C., Flanagan, L.B., Huemmrich, K.F., Kiddle, C., Sanchez-Azofeifa, G.A., Thayer, D.R., Vesco, L., Gianelle, D., Sims, D.A., Rahman, A.F., Pastorello, G.Z., 2010. SpecNet revisited: bridging flux and remote sensing communities. *Canadian Journal of Remote Sensing* 36, S376–S390.
- Gitelson, A.A., Merzlyak, M.N., 1994. Quantitative estimation of chlorophyll-a using reflectance spectra: experiments with autumn chestnut and maple leaves. *Journal of Photochemistry and Photobiology B: Biology* 22, 247–252.
- Gitelson, A.A., Merzlyak, M.N., 1997. Remote estimation of chlorophyll content in higher plant leaves. *International Journal of Remote Sensing* 18, 2691–2697.
- Gitelson, A.A., Kaufman, Y.J., Stark, R., Rundquist, D., 2002. Novel algorithms for remote estimation of vegetation fraction. *Remote Sensing of Environment* 80, 76–87.
- Gitelson, A.A., Gritz, Y., Merzlyak, M.N., 2003. Relationships between leaf chlorophyll content and spectral reflectance and algorithms for non-destructive chlorophyll assessment in higher plant leaves. *Journal of Plant Physiology* 160, 271–282.
- Gradowski, T., Thomas, S.C., 2006. Phosphorus limitation of sugar maple growth in central Ontario. *Forest Ecology and Management* 226 (1–3), 104–109.
- Guyot, G., Baret, F., 1988. Utilisation de la Haute Resolution Spectrale Pour Suivre l'etat des Couverts Vegetaux. Proceedings, 4th international colloquium "spectral signatures of objects in remote sensing. ESA Publication, SP-287, Paris, pp. 279–286 ESA, Aussois January 18–22.
- Haboudane, D., John, R., Millera, J.R., Tremblay, N., Zarco-Tejada, P.J., Dextraze, L., 2002. Integrated narrow-band vegetation indices for prediction of crop chlorophyll content for application to precision agriculture. *Remote Sensing of Environment* 81, 416–426.
- Haboudane, D., Miller, J.R., Pattey, E., Zarco-Tejada, P.J., Strachan, I.B., 2004. Hyperspectral vegetation indices and novel algorithms for predicting green LAI of crop canopies: modeling and validation in the context of precision agriculture. *Remote Sensing of Environment* 90, 337–352.
- Haboudane, D., Tremblay, N., Miller, J.R., Vigneault, P., 2008. Remote estimation of crop chlorophyll content using spectral indices derived from hyperspectral data. *IEEE Transactions on Geoscience and Remote Sensing* 46 (2), 423–437.
- Harron, J.W., 2000. Optical Properties of Phytoelements in Conifers. Graduate Program in Earth and Space Science. York University, Toronto, pp. 193 (M.Sc. Thesis).
- Inoue, Y., 2003. Synergy of remote sensing and modeling for estimating ecophysiological processes in plant production. *Plant Production Science* 6, 3–16.
- Jacquemoud, S., Baret, F., 1990. PROSPECT: a model of leaf optical properties spectra. *Remote Sensing of Environment* 34, 75–91.
- Jacquemoud, S., Ustin, S.L., 2001. Leaf optical properties: a state of the art. In: Proceedings of the 8th International Symposium Physical Measurements and Signatures in Remote Sensing, CNES, Aussois, France, pp. 223–232.
- Jordan, C.F., 1969. Derivation of leaf-area index from quality of light on the forest floor. *Ecology* 50, 663–666.
- Le Maire, G., François, C., Dufrêne, E., 2004. Towards universal broad leaf chlorophyll indices using PROSPECT simulated database and hyperspectral reflectance measurements. *Remote Sensing of Environment* 89, 1–28.

- Liu, J.G., Moore, J., 1990. Hue image RGB colour composition. A simple technique to suppress shadow and enhance spectral signature. *International Journal of Remote Sensing* 11 (8) 1521–1530.
- Maccioni, A., Agati, G., Mazzinghi, P., 2001. New vegetation indices for remote measurement of chlorophylls based on leaf directional reflectance spectra. *Journal of Photochemistry and Photobiology B: Biology* 61, 52–61.
- Main, R., Cho, M.A., Mathieu, R., O'Kennedy, M.M., Ramoelo, A., Koch, S., 2011. An investigation into robust spectral indices for leaf chlorophyll estimation. *ISPRS Photogrammetry and Remote Sensing* 66 (6) 751–761.
- McMurtrey III, J.E., Chappelle, E.W., Kim, M.S., Meisinger, J.J., Corp, L.A., 1994. Distinguishing nitrogen fertilization levels in field corn (*Zea mays* L.) with actively induced fluorescence and passive reflectance measurements. *Remote Sensing of Environment* 47, 36–44.
- Moorthy, I., Miller, J.R., Noland, T.L., 2008. Estimating chlorophyll concentration in conifer needles with hyperspectral data: an assessment at the needle and canopy level. *Remote Sensing of Environment* 112, 2824–2838.
- Mutanga, O., Skidmore, A.K., 2004. Narrow band vegetation indices overcome the saturation problem in biomass estimation. *International Journal of Remote Sensing* 25 (19) 3999–4014.
- Mutanga, O., Skidmore, A.K., 2007. Red edge shift and biochemical content in grass canopies. *ISPRS Journal of Photogrammetry and Remote Sensing* 62, 34–42.
- Ollinger, S.V., 2011. Sources of variability in canopy reflectance and the convergent properties of plants. *New Phytologist* 189, 375–394.
- Peñuelas, J., Baret, F., Filella, I., 1995. Semi-empirical indices to assess carotenoids/chlorophyll a ratio from leaf spectral reflectance. *Photosynthetica* 31, 221–230.
- Rayfield, B., Anand, M., Laurence, S., 2005. Assessing simple versus complex restoration strategies for industrially disturbed forests. *Restoration Ecology* 13 (4) 639–650.
- Richardson, A.D., Duigan, S.P., Berlyn, G.P., 2002. An evaluation of non-invasive methods to estimate foliar chlorophyll content. *New Phytologist* 153, 185–194.
- Richardson, A.D., Berlyn, G.P., Duigan, S.P., 2003. Reflectance of Alaskan black spruce and white spruce foliage in relation to elevation and latitude. *Tree Physiology* 23, 537–544.
- Rondeaux, G., Steven, M., Baret, F., 1996. Optimization of soil -adjusted vegetation index. *Remote Sensing of Environment* 24, 109–127.
- Rouse, J.W., Haas, R.H., Schell, J.A., Deering, D.W., Harlan, J.C., 1974. Monitoring the vernal advancement and retrogradation (greenwave effect) of natural vegetation. NASA/GSFC Type III Final Report. NASA, Greenbelt, MD, pp. 371.
- Rowe, J.S., 1972. Forest regions of Canada. Publication 1300. Department of the Environment, Canadian Forestry Service, Ottawa, pp. 172.
- Sampson, P.H., Zarco-Tejada, P.J., Mohammed, G.H., Miller, J.R., Noland, T.L., 2003. Hyperspectral remote sensing of forest condition: estimating chlorophyll content in tolerant hardwoods. *Forest Science* 49, 381–391.
- Serrano, L., 2008. Effects of leaf structure on reflectance estimates of chlorophyll content. *International Journal of Remote Sensing* 29 (17–18) 5265–5274.
- Simic, A., Chen, J.M., Noland, T.L., 2011. Retrieval of forest chlorophyll content using canopy structure parameters derived from multi-angle data: the measurement concept of combining nadir hyperspectral and off-nadir multispectral data. *International Journal of Remote Sensing* 32 (20) 5621–5644.
- Sims, D.A., Gamon, J.A., 2002. Relationships between leaf pigment content and spectral reflectance across a wide range of species, leaf structures and developmental stages. *Remote Sensing of Environment* 81, 337–354.
- Smith, R.C., Adams, J., Stephens, D.J., Hick, P.T., 1995. Forecasting wheat yield in a Mediterranean-type environment from the NOAA satellite. *Australian Journal of Agricultural Research* 46, 113–125.
- Ustin, S.L., Roberts, D.A., Gamon, J.A., Asner, G.P., Green, R.O., 2004. Using imaging spectroscopy to study ecosystem processes and properties. *Bioscience* 54, 523–534.
- Verrelst, J., Schaepman, M.E., Clevers, J.G.P.W., 2008. A modelling approach for studying forest chlorophyll content in relation to canopy composition. In: Proceedings of the XXI ISPRS Congress on the International Archives of Photogrammetry. Remote Sensing and Spatial Information Sciences (ISPRS), Beijing, China, 3–11 July 2008 (Beijing: ISPRS, 2008 (3), 25–30).
- Vogelmann, J.E., Rock, B.N., Moss, D.M., 1993. Red-edge spectral measurements of sugar maple leaves. *International Journal of Remote Sensing* 14 (9) 1563–1575.
- Wu, C., Niu, Z., Tang, Q., Huang, W., 2008. Estimating chlorophyll content from hyperspectral vegetation indices: modeling and validation. *Agricultural Forest Meteorology* 148 (8–9) 1230–1241.
- Zarco-Tejada, P.J., Miller, J.R., Noland, T.L., Mohammed, G.H., Sampson, P.H., 2001. Scaling-up and model inversion methods with narrowband optical indices for chlorophyll content estimation in closed forest canopies with hyperspectral data. *IEEE Transactions on Geoscience and Remote Sensing* 39, 1491–1507.
- Zarco-Tejada, P.J., Miller, J.R., Harron, J., Hu, B., Noland, T.L., Goel, N., et al., 2004. Needle chlorophyll content estimation through model inversion using hyperspectral data from boreal conifer forest canopies. *Remote Sensing of Environment* 89, 189–199.
- Zarco-Tejada, P.J., Berjón, A., López-Lozano, R., Miller, J.R., Martín, P., Cachorro, V., et al., 2005. Assessing vineyard condition with hyperspectral indices: leaf and canopy reflectance simulation in a row-structured discontinuous canopy. *Remote Sensing of Environment* 99, 271–287.
- Zhang, Y., Chen, J.M., Thomas, S.C., 2007. Retrieving seasonal variation in chlorophyll content of overstorey and understorey sugar maple leaves from leaf-level hyperspectral data. *Canadian Journal of Remote Sensing* 5, 406–415.
- Zhang, Y., Chen, J.M., Miller, J.R., Noland, T.L., 2008a. Retrieving chlorophyll content of conifer needles from hyperspectral measurements. *Canadian Journal of Remote Sensing* 34, 296–310.
- Zhang, Y., Chen, J.M., Miller, J.R., Noland, T.L., 2008b. Leaf chlorophyll content retrieval from airborne hyperspectral remote sensing imagery. *Remote Sensing of Environment* 112, 3234–3247.